JOURNAL OF MATERIALS SCIENCE 8 (1973) 1238–1246

The creep of sapphire filament with orientations close to the *c*-axis

D. J. GOOCH*, G. W. GROVES
Department of Metallurgy, University of Oxford, UK

Sapphire filament oriented within $2\frac{1}{2}°$ of the crystallographic *c*-axis underwent creep by a mechanism other than slip on the basal planes at temperatures above 1600°C. There was a stress below which creep could not be detected; this decreased from 180 MNm^{-2} at 1600°C to 65 MNm^{-2} at 1800°C. The total tensile strain obtained never exceeded 5%. Fracture occurred during a linear stage of creep in which the stress exponent of the strain-rate was approximately 6. The creep mechanism appeared to be slip on $\{20\bar{2}\bar{1}\}$ $\langle 01\bar{1}2\rangle$ (morphological unit cell). A filament in which the *c*-axis lay at 6° to the filament axis deformed by localized basal slip. The accompanying local latice rotations produced fracture at a small overall strain, usually less than 0.5%. The results demonstrate extreme anisotropy of creep in sapphire crystals.

1. Introduction

The mechanical properties of single-crystal aluminium oxide (sapphire) have attracted considerable attention because of its high strength and its stability in air at temperatures up to its melting point (2050°C). Above 900°C, large-scale plastic deformation can occur by glide on the basal planes [1, 2] but by orienting the *c*-axis of the crystal parallel to the tensile axis, slip on these planes can be prevented. We shall refer to specimens tested in this orientation as 0° specimens. Small extensions in creep have been obtained from 0° rods grown by the Verneuil process at a temperature of 1600°C and stresses of approximately 100 MNm^{-2} [3]. Sapphire filament with the *c*-axis approximately parallel to the axis of the filament is now available commercially†, and Shahinian [4] has reported the results of creep tests of this material at 1700 and 1900°C. The present work is a more detailed study of the creep and fracture of the filament in the temperature range 1600 to 1800°C and of the contrasting properties of a filament in which the *c*-axis lay at an angle of 6° to the axis of the filament.

2. Experimental procedures

The sapphire filament was nominally 0.25 mm in diameter. Specimens were prepared from five batches of filament which were found to have the *c*-axis at the following angles to the filament axis $\frac{1}{2}° \pm \frac{1}{2}°$, $1\frac{1}{2}° \pm \frac{1}{2}$, $2° \pm \frac{1}{2}°$, $2\frac{1}{2}° \pm \frac{1}{2}°$, $6° \pm 1°$. The filaments contained a large number of small voids ($\sim$ 1 μm diameter) which are thought to be produced by thermal contraction during the growth process [5].

Tensile creep tests were carried out in an air-atmosphere furnace with a recrystallized alumina tube, open at both ends so that the ends of a filament could be gripped outside the furnace. Creep extensions were measured with an LVDT giving a sensitivity of 0.01% in strain detection. After testing, filaments were etched to reveal dislocations by a modification of the method described by Scheuplin and Gibbs [6]. Pieces of filament were placed in concentrated orthophosphoric acid in a platinum crucible, heated rapidly to 500°C and then allowed to cool to room temperature. This method produced dislocation etch pits at all orientations of the filament surface. Thin foils for electron microscopy were prepared by mechanical polishing, followed by ion beam thinning.

In calculating creep strains, a major problem lay in accounting for deformation occurring outside the hot zone, in which the temperature was constant to within 3°C over a length of approximately 25 mm. (The accuracy of measure-

*Now at C.E.R.L., Leatherhead, UK.
†The Tyco Laboratories Inc, Waltham, Mass, USA.

ment of the hot-zone temperature was $\pm 5°C$.) The temperature profile of the furnace could be approximated by

$$T = T_c \text{ for } |x| < 12.5 \text{ mm}$$
$$T = T_c - 2(|x| - 12.5) \text{ for } |x| > 12.5 \text{ mm} \quad \ldots\ldots (1)$$

where T is the temperature in °C at a distance $|x|$ from the centre of the furnace. An effective gauge length can be defined as the length by which the total creep extension rate must be divided to give the correct value of the strain rate within the hot zone. The effective gauge length was estimated by assuming that above a critical temperature the creep rate was of the form

$$\dot{\epsilon} = A \exp - Q/RT \qquad (2)$$

where A is a constant at a given stress. It was assumed that no creep occurred below the critical temperature T_0. Then the effective gauge length l is given by

$$l = \frac{\dot{e}}{\dot{\epsilon}_c} = 25 + 2\frac{\int_{x_0}^{12.5} \exp - Q/RT\,dx}{\exp - Q/RT_c} \qquad (3)$$

where $\dot{e}$ is the extension rate of the filament and x_0 the distance from the centre of the furnace of the critical temperature T_0. Effective gauge lengths were calculated from Equation 3 using the values of T_0 obtained from the observed creep yield stresses (Table I) and an activation energy Q of 180 kcal mol^{-1} (the value obtained by Chang [7] from measurements of creep in sapphire deforming by basal slip). Values of the order of twice the hot-zone length were obtained at temperatures and stresses well above the threshold levels. At stresses in excess of about 30 MNm^{-2} above the creep yield stress, the effective gauge length shows only a small further increase with increasing stress, so that any uncertainty in the absolute value of the strain rate arising from the estimation of an effective gauge length should not introduce serious error into the determination of the stress dependence of the creep rate at such stresses. At temperatures above 1650°C and stresses above 140 MNm^{-2}, the temperature dependence of the effective gauge length is also small, so that significant error in the determination of the temperature dependence of the creep rate can also be avoided.

3. Results

3.1. Specimens not exhibiting basal deformation

3.1.1. Creep behaviour

Specimens which did not deform by basal slip were the $\frac{1}{2}°$, $1\frac{1}{2}°$, 2°, and $2\frac{1}{2}°$ filaments, these will in future be referred to as 0° specimens. Typical creep curves are shown in Fig. 1. There was generally an initial transient of increasing creep rate followed by a period of constant rate. At the lower stresses the period of increasing rate was followed by a decrease leading to an undetectable rate. The initial transient was generally over after an extension of less than 0.5%. Failure of the specimens occurred during the period of linear creep, not by a single fracture but by the specimen fracturing at up to a dozen places along its length. The amount of plastic strain before failure appeared to be random and was not a reproducible function of stress and temperature, although in general the larger strains were observed at the higher temperatures and strain-rates, the maximum strain being approximately 5%.

3.1.2. Stress dependence

At each test temperature between 1600 and 1800°C there was a critical stress level below which no creep was detected after a period of 50 h. These stress levels are given in Table I. (The upper limit to the value of the creep rate at the "creep yield stress", set by the sensitivity of the apparatus, is on the order of 10^{-9} sec^{-1}.) Below 1600°C, the specimens always fractured before any creep strain was detectable. A very

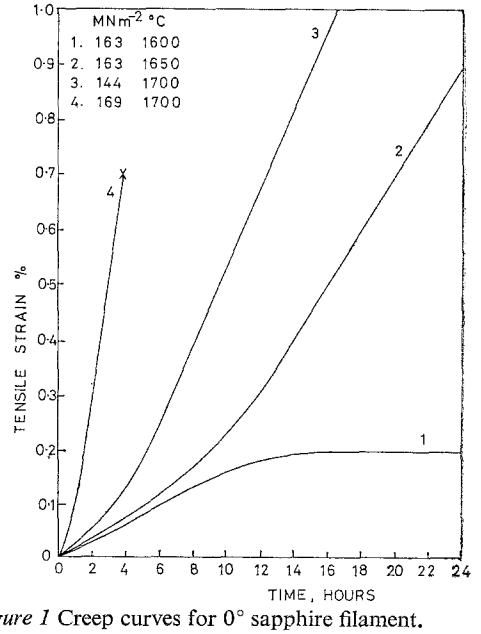

Figure 1 Creep curves for 0° sapphire filament.

TABLE I Yield stresses and stress exponents for the creep of 0° sapphire filament.

Temperature °C	Creep yield stress, MN m^{-2}	Stress exponent, n
1600	170	—
1650	140	6.9 ± 0.3
1700	110	6.8 ± 0.2
1750	85	5.7 ± 0.3
1800	65	6.1 ± 0.1

marked stress dependence of the linear creep rate was observed, but tests on different specimens, even from the same filament batch showed considerable scatter. To overcome this difficulty stress change experiments were carried out within the linear creep stage. An increase of stress produced a new constant creep rate, with occasionally a short transient, but when the stress was reduced to a previous value after several increments the strain-rate did not return to its previous value at that stress but to a somewhat higher value. The results shown in Fig. 2 represent the effect of increasing the stress. On a log (stress) log (strain-rate) plot, good straight lines are obtained at stresses above the creep

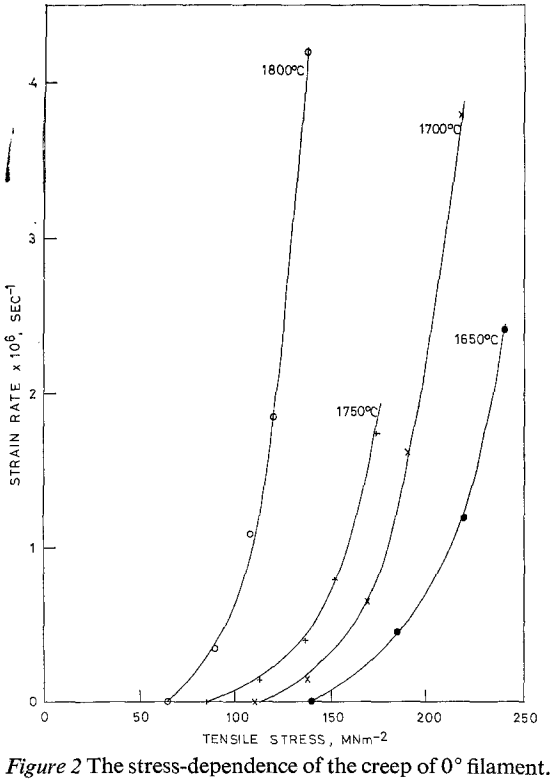

Figure 2 The stress-dependence of the creep of 0° filament. The curves show the effect on the strain rate of increasing the stress during the linear part of the creep curve.

yield stress and the values of the slopes d log $\dot{\epsilon}$/d log σ are shown in Table I. The linear strain-rate is seen to be highly stress-dependent, and the effect of increasing stresses can be described by an equation of the form

$$\dot{\epsilon} = a\,\sigma^n \qquad (4)$$

with n in the range of approximately 6 to 7.

3.1.3. Temperature dependence

Tests were conducted in which the test temperature was increased while the specimen was deforming in the constant creep rate region. Since the temperature control on the furnace allowed the required temperature to be overshot by ~ 15°C before equilibrium was reached it was necessary to unload the specimen while the temperature was being raised. It usually took approximately 10 min to reach a new equilibrium temperature 25°C above the first, during which time the specimen was kept loaded at a stress well below the creep yield stress at the higher temperature.

Measurements of creep rates were always made during the region of linear creep. Due to the limited ductility of the specimens and the low range of temperatures over which linear creep occurred for a given stress level, the maximum number of values obtainable for any one specimen was five. Sometimes it was possible to take only three readings, especially at the higher stress levels.

Fig. 3 shows the variation of creep rate with temperature plotted as $\log_{10}$ (creep rate) against $1/T$ K. Line A ($\frac{1}{2}$°, 132 MNm^{-2}) is a composite curve made up from two points from each of two different tests. Likewise, line B ($1\frac{1}{2}$° 193 MNm^{-2}) is a composite curve from values obtained from several individual tests.

The values of the apparent activation energy, Q, decrease as the stress level is increased, from 310 kcal mol^{-1} at 132 MNm^{-2} to 200 kcal mol^{-1} at 204 MNm^{-2}. There was no significant difference between $1\frac{1}{2}$°, 2° and $2\frac{1}{2}$° specimens. A small batch of $\frac{1}{2}$° filament gave an anomalously low apparent activation energy of 130 kcal mol^{-1} at 132 MNm^{-2}.

3.1.4. Physical examination

A whitening of the filament outside the hot zone was observed. The whitening was seen on specimens tested in argon, nitrogen, hydrogen and oxygen, as well as on specimens tested in air. It was thought to be due to the formation of voids,

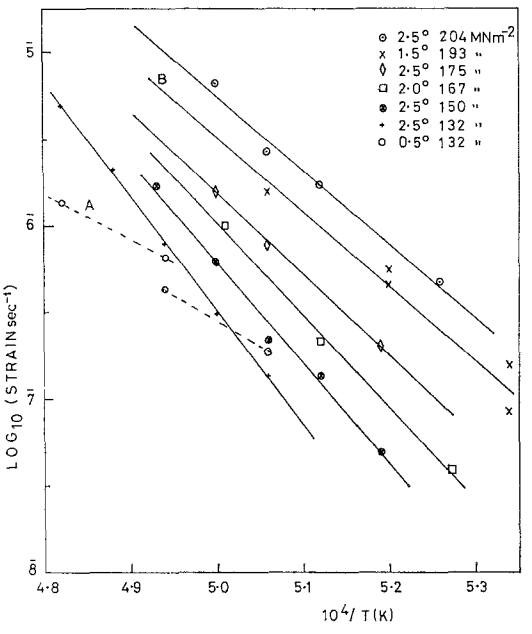

Figure 3 Temperature dependence of the creep rate in the linear part of the creep curve of 0° filament.

which were observed by transmission electron microscopy to be disc-shaped, lying parallel to (0001) planes and typically 0.5 μm in diameter. In the regions of highest concentration their volume fraction was on the order of 3×10^{-3}. Although dislocations were occasionally seen to be associated with them, they were not a result of plasticity since they were observed in specimens loaded below the creep yield stress.

Filament from within the hot zone often showed crystallographic striations on $\{10\bar{1}0\}$ orientations of the surface. The striations varied considerably in form, as shown in Fig. 4. Laue photographs showed that they corresponded to the traces of $\{10\bar{1}x\}$ rather than $\{10\bar{1}x\}$ planes.* Measurements of the plane of the striations from the curvature of the more sharply defined striations gave agreement with $\{20\bar{2}\bar{1}\}$ planes, within a scatter of measurement of $\pm 10°$. The striations often took the form of sharp notches, and it is thought probable that they acted as stress concentrators leading to the failure of the filament by a delayed brittle fracture.

Fracture surfaces usually showed a fracture origin at a region of the filament surface close to the $\{10\bar{1}0\}$ orientation, in agreement with this. Fig. 5 shows a fracture surface containing two regions, one parallel to (0001) containing steps radiating from the fracture origin at the surface, and a region of final cleavage on a non-basal plane.

When deformed filaments were etched, some regions of high etch-pit density were found ($\sim 10^7$ cm^{-2}) and no clear linear arrangements could be detected in these regions. In other, presumably less heavily deformed regions, lines of pits could be seen (Fig. 6). The orientation of these lines was consistent to within $\pm 10°$ with $\{20\bar{2}\bar{1}\}$ planes. There was no clear correlation between the etch pit patterns and the striations described above.

Transmission electron microscope specimens were obtained but in the areas sampled the dislocation density was too low to give useful information on the dislocation arrangements. Diffraction contrast experiments indicated the presence of both $\frac{1}{3}\langle 11\bar{2}0\rangle$ and $\frac{1}{3}\langle 01\bar{1}2\rangle$ Burgers vectors.

3.2. Specimens exhibiting basal deformation

3.2.1. Creep behaviour

The behaviour of the 6° sapphire filament was quite different from that classed as 0° filament, i.e. $\frac{1}{2}°$, $1\frac{1}{2}°$, 2° and $2\frac{1}{2}°$.

For a given temperature there was a definite stress level below which no plastic extension (apart from an occasional short transient) was detected over a period of approximately 50 h. The variation of this stress level with temperature is shown in Table II. Above the "creep yield stress", plastic deformation was observed but the elongation of the specimens was severely limited by the mode of deformation and the final failure. In the temperature range 1600 to 1700°C an approximately linear variation of tensile strain with time was observed for the 6° filament, sometimes after an initial decreasing transient. There appeared to be no consistent variation in the form of the transient and it was assumed that it depended upon the original dislocation structure of the filament.

The period of constant strain-rate was very limited and never resulted in a tensile strain greater than 0.2%. This period was then followed by one of rapidly increasing rate up to the final failure point. Fracture was in all cases at a single point as opposed to the shattering observed in 0° specimens. Fig. 7 shows typical creep curves and illustrates that much of the total extension occurred during the final period of increasing strain-rate. Because of the limited

*The morphological unit cell, $c = 6.5$Å is used.

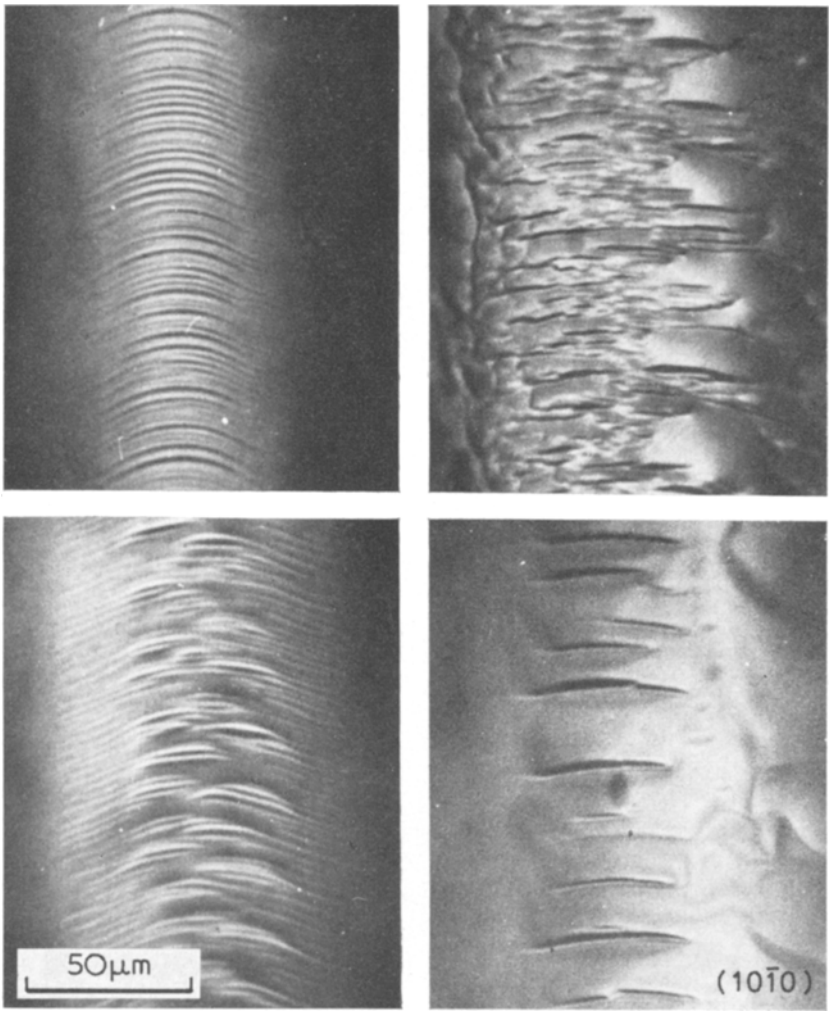

Figure 4 Surface markings on creep-tested 0° filaments. The filament axis is vertical in each case.

ductility it was not possible to make a detailed analysis of the variation of linear strain-rate with stress and temperature.

Increasing the test temperature to 1750°C gave similar strain-time curves to those between 1600 and 1700°C except that it was possible to obtain greater tensile elongations (up to 0.5%) during the linear region. At 1800°C, however, the behaviour was quite different The linear creep period resulted in tensile elongations of over 1%, comparable with the elongations observed for 0° specimens. Only two specimens were available to be tested at this temperature. The first was tested at 55 MNm^{-2} and still had not failed after 50 h with an extension of 0.5%. The second specimen was first loaded to 65 MNm^{-2} for 70 h, then 75 MNm^{-2} for 24 h and finally to 85 MNm^{-2} at which stress it failed after 5 h with an elongation of 1.2% during the summed linear creep regions. The final failure was preceded by a short increasing rate period.

3.2.2. Physical examination

In the temperature range 1600 to 1700°C, fracture of the 6° filament was associated in each specimen with a kink as shown in Fig. 8a. The structure of a kinked region is illustrated in Fig. 9. Massive basal slip has occurred in regions B, resulting in lattice rotations of up to 20°. Region C has not deformed and has rotated in bulk in order to maintain a coherent interface with the deformed regions. The fact that the kinked region itself was undeformed was seen by the absence of slip lines, whereas the deformed

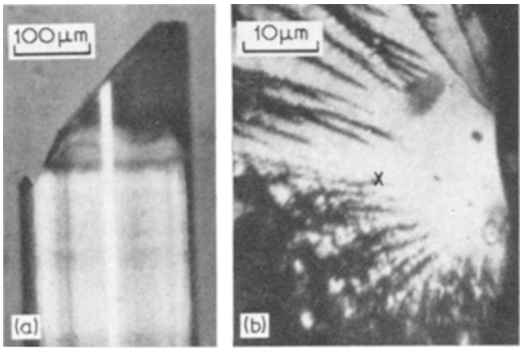

Figure 5 Fracture surface of 0° filament fractured in creep; (a) side view of fracture surface, (b) enlarged view of fracture origin.

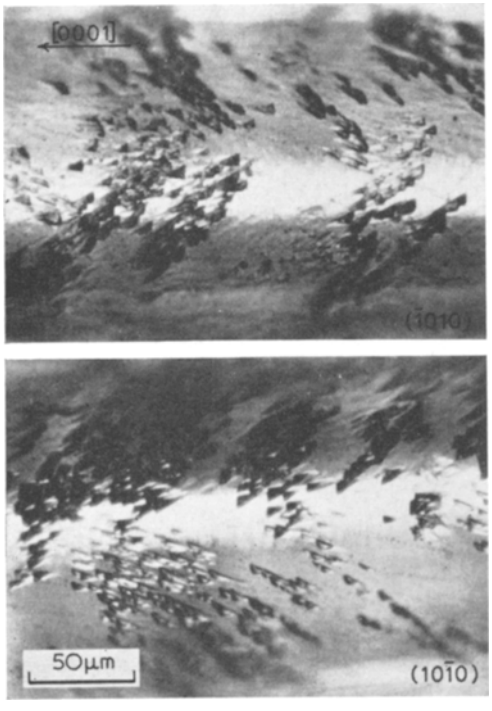

Figure 6 Etch pits produced by phosphoric acid on the surface of a 0° filament after creep deformation.

region was covered in slip lines parallel to the rotated basal planes. Etching in orthophosphoric acid confirmed this since the deformed region produced etch pits lined up along the basal planes whereas the kinked region produced no more pits than the untested filament.

The boundary between the deformed regions B and the undeformed regions A, was formed by a band of closely spaced low angle boundaries (Fig. 8b). Where these intersected the filament surface, cracks started to open (Fig. 10) and it

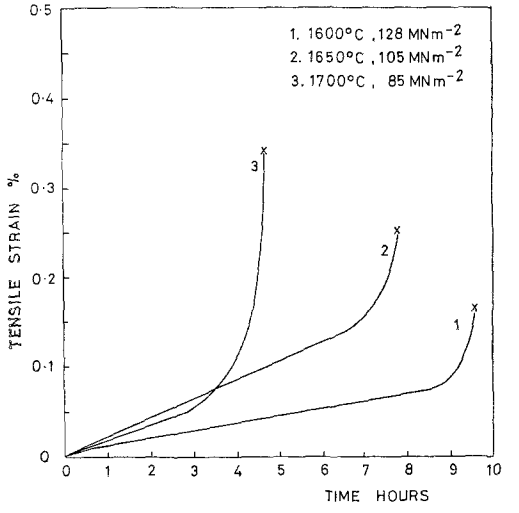

Figure 7 Creep curves for 6° filament.

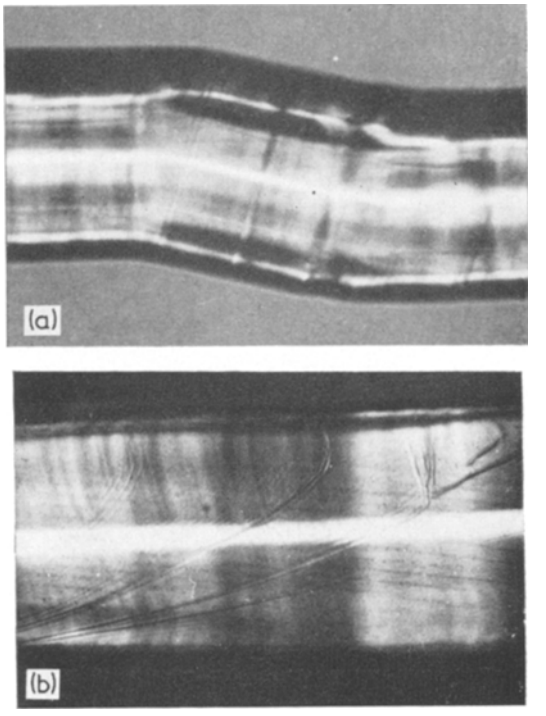

Figure 8 (a) Kink in 6° filament deformed by creep at 1650°C. (b) Boundary of a region having undergone basal slip. The basal slip lines are faintly visible in the upper left hand region, which is bounded by tilt boundaries which can be seen through a thermal grooving effect.

was these that resulted in the ultimate failure. Propagation of the cracks was along the path of one of the low angle boundaries.

Specimens deformed at 1750°C still showed

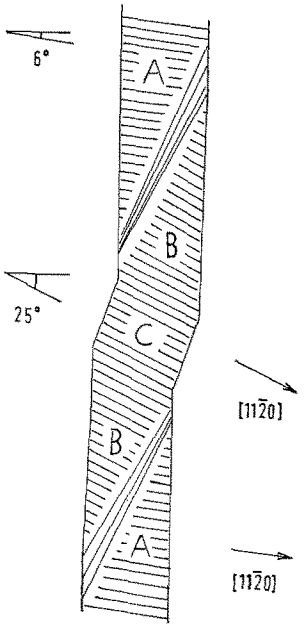

Figure 9 The structure of a kinked region.

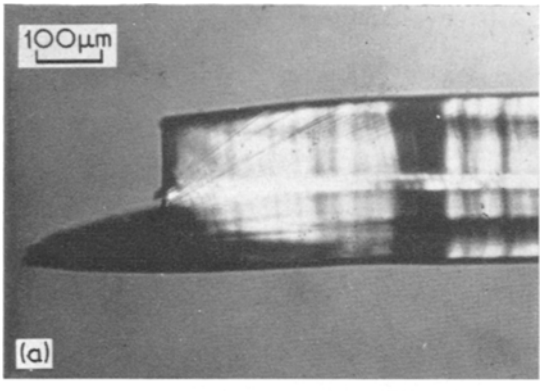

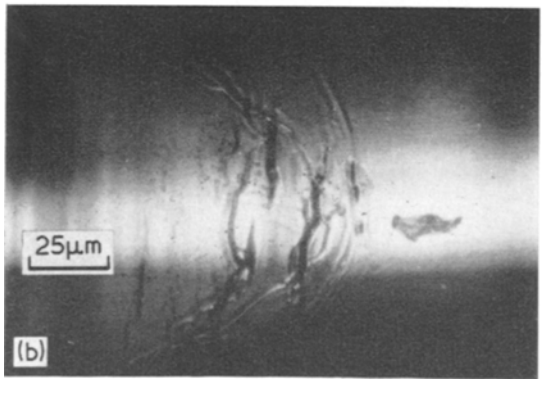

Figure 10 (a) Fracture surface of a 6° filament (side view). (b) Microcracks formed at the surface of the filament in the region where the part having undergone slip is bounded by tilt boundaries.

TABLE II Creep yield stresses for 6° sapphire filament.

Temperature, °C	Creep yield stress, MN m^{-2}
1600	120
1650	95
1700	70
1750	50

some evidence of the kinking phenomenon, except that sometimes the actual kink was absent, leaving only the deformed region, bounded at either end by the low-angle boundaries.

At 1800°C ultimate failure was by a process of basal necking over a very limited region; this was thought to be associated with the final period of increasing creep rate.

Both specimens tested at 1800°C had the same crystallographic striations seen on the 0° specimens; once again however, there was no correlation between the striations and etch pits produced by orthophosphoric acid. As in the 0° specimens the etch pits were lined up in arrays consistent with the $\{20\bar{2}\bar{1}\}$ planes. Neither the striations nor the etch pit patterns were seen on 6° specimens deformed between 1600 and 1750°C.

The tilt boundaries bounding regions having undergone basal slip at 1600 to 1750°C were examined more closely by transmission electron microscopy. Walls of regularly spaced edge dislocations of $\frac{1}{3}\langle 11\bar{2}0\rangle$ Burgers vector were seen (Fig. 11). Tilt angles of between 0.05° and 0.3° were calculated from the dislocation spacing.

4. Discussion

An initially increasing creep rate, as shown by 0° sapphire filaments, is not an uncommon observation in non-metals. Sapphire oriented to allow basal slip gives similar creep curves at temperatures between 900 and 1200°C [3]. In this case, the creep curve is sigmoidal, i.e., the linear stage is followed by one of decreasing strain rate. Sigmoidal creep has been reported in other non-metals, such as silicon [8] germanium [9] and lithium fluoride [10]. In these cases it has been suggested that the initial increase of creep rate is due to dislocation multiplication and it is probable that this explanation applies also to 0° sapphire. On the other hand catastrophic acceleration of the creep rate observed in the final stages of the creep curve of 6° filament (Fig. 7) can be attributed to a geometrical softening due to the rotation of the basal slip plane, of

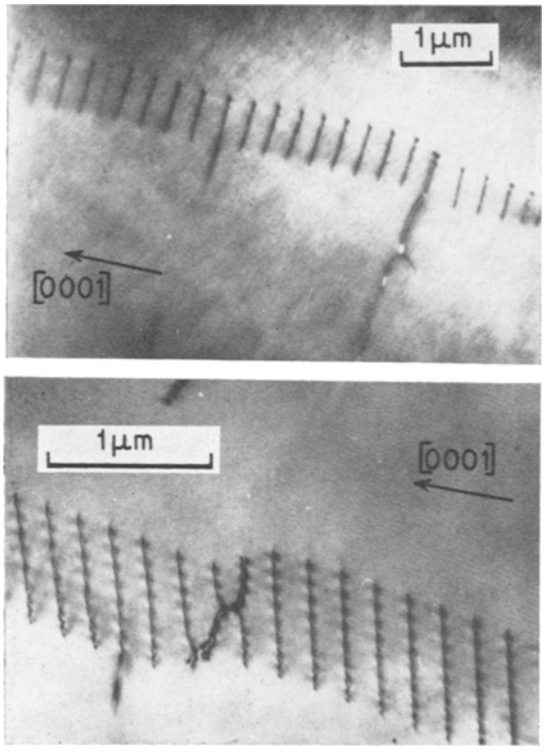

Figure 11 Dislocation structure of the tilt boundaries formed as a result of basal plane slip in 6° filament.

the same type as that reported in zinc [11]. In sigmoidal creep, the decreasing creep rate stage is usually attributed to work-hardening. The absence of this stage in 0° filament may be due simply to the intervention of brittle fracture. However, the fairly large extent of the linear creep following the initial acceleration in some cases makes it necessary to examine the possibility that it is a steady-state creep occurring by one of the known mechanisms. The most frequently quoted creep model, due to Weertman [12] of dislocation glide rate-controlled by a climb process predicts an activation energy equal to that for self-diffusion, in the case of Al_2O_3 presumably of the larger O^{2-} ion. The observed apparent activation energy at low stresses is however about twice that of 152 kcal mol^{-1}, for the self diffusion of O^{2-} [14]. The same difficulty applies to the steady-state model due to Nabarro [13], in which the strain is produced directly by dislocation climb. Furthermore the observed stress dependence is considerably higher than that predicted by the Nabarro model (stress exponent $n = 3$ if diffusion is through the lattice and $n = 5$ if diffusion is along dislocation cores).

It is perhaps more plausible that the creep mechanism is dislocation glide, rate-controlled by the thermally activated overcoming of a Peierls barrier to slip on a difficult system, for example $\{20\bar{2}\bar{1}\}\langle 01\bar{1}2\rangle$. Some aspects of the results favour this interpretation.

If activation volumes are calculated from the changes in strain-rate produced by stress increments, they do lie in the range 10 $\boldsymbol{b}^3$ to 100 $\boldsymbol{b}^3$, where $\boldsymbol{b}$ is the Burgers vector, assumed to be $\frac{1}{3}\langle 01\bar{1}2\rangle$, as expected for Peierls stress control [18]. The observation that the apparent activation energy decreases with stress (Fig. 3) is qualitatively consistent with theories of the thermally activated glide of dislocations [18, 19]. However, it is not possible to interpret the apparent activation energies as energy barriers to thermally activated glide because of their large magnitude. Thus, the Weertman model of creep controlled by the Peierls stress [16] predicts a strain rate too small by many orders of magnitude when the observed activation energies are inserted. Similarly, the application of more recent expressions for the strain rate due to thermally activated glide [18, 19] requires implausibly large pre-exponential factors if the observed activation energy is taken to be the energy barrier to be overcome during glide. Activation energies higher than that for self-diffusion have been reported previously in studies of the creep of zinc [15], and attributed to the operation of a difficult slip system, but in the case of 0° sapphire it appears more likely that the high apparent activation energies arise from structural changes (changes in dislocation configuration or impurity state) which occur when the temperature is changed. It follows that neither the value of the apparent activation energy nor its stress dependence can be interpreted directly in terms of a Peierls barrier. The physical examination of deformed filaments indicates that the deformation mechanism is dislocation glide. The alignments of etch-pits suggest the $\{20\bar{2}\bar{1}\}\langle 01\bar{1}2\rangle$ slip system.

The origin of the striations which correspond with the intersection of $\{20\bar{2}\bar{1}\}$ planes with $\{10\bar{1}0\}$ regions of the filament surface is not clear, but the considerable depth of many of them suggests that thermal etching rather than slip plays the major role in their formation. They are of importance in that they appear to provide the surface stress concentrations leading to the fracture of 0° filaments.

The extreme anisotropy of creep in sapphire

crystals becomes apparent when the creep yield stresses reported in Table I are compared with those found by Wachtman and Maxwell [17] in crystals oriented to favour basal slip. They found yield stresses, resolved onto the basal plane, ranging from 78 MNm^{-2} at 900°C to 13 MNm^{-2} at 1400°C. Another manifestation of this anisotropy is the complete change of behaviour which occurs when the orientation of the filament departs by only 6° from the *c*-axis. At temperatures in the range 1600 to 1700°C, the 6° filament deforms entirely by basal slip, which leads to large local lattice rotations. Although large local shear strains (as high as 40%) occur, the filament fractures when the overall strain is still small, probably as a result of bending stresses set up by the local lattice rotations. The initiation of fracture at the edge of a deformed region (Fig. 10) may be explained by the stress-concentrating effect of thermal grooves produced along the intersection of the tilt boundaries with the surface; which are clearly visible in Figs. 8 and 10. At a temperature of 1800°C, there was evidence of a mixture of basal and non-basal slip suggesting that above 1800°C, the easier operation of pyramidal slip systems may remove the striking difference between the behaviour of 6° and 0° filament which is observed at lower temperatures.

5. Summary and conclusions

Creep strains of a few per cent, not occurring by slip on the basal plane, are obtained at temperatures above 1600°C in sapphire filament oriented within $2\frac{1}{2}°$ of the *c*-axis. An initial acceleration of the creep rate, attributed to dislocation multiplication, is followed by a linear stage ending in a brittle fracture at a total strain of a few per cent. The creep rate within the linear stage is highly sensitive to stress and temperature changes. Stress increases produce strain-rates proportional to the applied stress to a power of approximately 6. The temperature dependence corresponds to an activation energy decreasing with stress, and always in excess of the activation energy for the diffusion of the oxygen ion. The deformation mechanism was not conclusively established, but there is evidence for slip on the $\{20\bar{2}\bar{1}\}\langle 01\bar{1}2\rangle$ system. Fractures appeared to initiate at the filament surface where steps due primarily to thermal etching had developed. Filament misoriented by 6° from the *c*-axis underwent slip on the basal plane. The creep rate increased rapidly before fracture due to the rotation of the basal planes into an increasingly favourable orientation. Stress associated with the occurrence of this lattice rotation in local regions leads to fracture at small overall strains at temperatures in the range 1600 to 1700°C; at 1800°C some non-basal slip occurs, allowing larger strains before fracture.

Acknowledgements

The authors acknowledge with gratitude support from the National Physical Laboratory, Teddington and UKAERE Harwell during the course of this work.

References

1. M. L. KRONBERG, *Acta Metallurgica* **5** (1957) 507.
2. H. CONRAD, *J. Amer. Ceram. Soc.* **48** (1965) 195.
3. J. B. WACHTMAN and L. H. MAXWELL, *ibid* **40** (1957) 377.
4. P. SHAHINIAN, *ibid* **54** (1957) 377.
5. J. T. A. POLLOCK, *J. Mater. Sci.* **7** (1972) 631.
6. R. SCHEUPLIN and P. GIBBS, *J. Amer. Ceram. Soc.* **43** (1960) 458.
7. R. CHANG, *J. Appl. Phys.* **31** (1960) 484.
8. M. M. MYSHLYAEV and V. I. NITITENKO, *Soc. Phys. Doklady* **14** (1970) 685.
9. K. BERNER and H. ALEXANDER, *Acta Metallurgica* **15** (1967) 933.
10. W. A. COGHLAN, R. A. MENEZES, and W. D. NIX, *Phil. Mag.* **23** (1971) 1515.
11. A. H. COTTRELL and V. AYTEKIN, *J. Inst. Metals* **77** (1950) 389.
12. J. WEERTMAN, *J. Appl. Phys.* **28** (1957) 362.
13. F. R. N. NABARRO, *Phil. Mag.* **16** (1967) 231.
14. Y. OISHI and W. D. KINGERY, *J. Chem. Phys.* **33** (1960) 480.
15. W. J. M. TEGART and O. D. SHERBY, *Phil. Mag.* **3** (1958) 1287.
16. J. WEERTMAN, *J. Appl. Phys.* **28** (1957) 1185.
17. J. B. WACHTMAN and L. H. MAXWELL, *J. Amer. Ceram. Soc.* **37** (1954) 291.
18. P. GUYOT and J. E. DORN, *Canad. J. Phys.* **45** (1967) 983.
19. M. S. DUESBERY, *Phil. Mag.* **19** (1969) 501.

Received 10 January and accepted 25 January 1973.